Multi-quasiparticle isomers involving proton-particle and neutron-hole configurations in ^{131}I and ^{133}I

H. Watanabe,[1,*] G. J. Lane,[1] G. D. Dracoulis,[1] A. P. Byrne,[1] P. Nieminen,[1,†] F. G. Kondev,[2] K. Ogawa,[3]
M. P. Carpenter,[4] R. V. F. Janssens,[4] T. Lauritsen,[4] D. Seweryniak,[4] S. Zhu,[4] and P. Chowdhury[5]

[1]*Department of Nuclear Physics, Research School of Physical Sciences and Engineering, Australian National University, Canberra, A.C.T. 0200, Australia*
[2]*Nuclear Engineering Division, Argonne National Laboratory, Argonne, Illinois 60439, USA*
[3]*Nuclear Physics Research Division, RIKEN Nishina Center, 2-1 Hirosawa, Wako, Saitama 351-0198, Japan*
[4]*Physics Division, Argonne National Laboratory, Argonne, Illinois 60439, USA*
[5]*Department of Physics, University of Massachusetts, Lowell, Massachusetts 01854, USA*
(Received 15 April 2009; published 11 June 2009)

The nuclei ^{131}I and ^{133}I have been populated in multinucleon transfer reactions between ^{136}Xe ions and various targets, and their structure has been investigated by time-correlated γ-ray coincidence spectroscopy and the measurement of γ-ray angular correlations. A $19/2^-$ isomer at 1918 keV, with a half-life of 24(1) μs, has been identified in ^{131}I, as well as nanosecond isomers with $J^\pi = 23/2^+$ in both isotopes. A $T_{1/2} = 25(3)$ ns isomer at 4308 keV in ^{131}I is suggested to have $J^\pi = (31/2^-, 33/2^-)$ and is primarily attributed to the coupling of an odd proton in the $d_{5/2}$ or $g_{7/2}$ orbit with the $(\pi^2)_{0^+}(\nu h_{11/2}^{-3} d_{3/2}^{-1})_{15^-}$ configuration in ^{130}Te responsible for the 15^- isomer in that nucleus. The observed level properties are compared with predictions of a shell-model calculation.

I. INTRODUCTION

The iodine isotopes with $Z = 53$ and three valence protons outside the $Z = 50$ shell closure have attracted considerable interest because they exhibit a transition from more collective nature in the middle of the neutron shell to spherical shell-model structure as the number of neutrons increases toward the $N = 82$ closed shell. Systematic experimental investigations of high-spin states using heavy-ion-induced fusion-evaporation reactions have revealed the collective properties of the odd-A isotopes up to ^{127}I [1–3]. At the other extreme, the excited states in the closed neutron-shell isotope ^{135}I can be described well in terms of three-proton configurations, except for the levels above 4.2 MeV that involve the valence protons coupled to particle-hole excitations across the $N = 82$ shell closure [4]. Because ^{135}I is neutron rich, it cannot be populated in conventional fusion-evaporation reactions using stable beams and targets. Hence, several authors [4–6] have exploited fission of ^{248}Cm. The nuclei between these two extremes are expected to exhibit a coexistence of collective and shell-model structures, although spectroscopic information on the excited states is limited so far to information obtained in β-decay studies [7–9].

In the present work, we have populated excited states in ^{131}I$_{78}$ and ^{133}I$_{80}$ using multinucleon transfer from ^{136}Xe, with the aim of understanding the effect of neutron holes on nuclear structure. In addition to previously known isomeric states with

$J^\pi = 15/2^-$ and $19/2^-$ in ^{131}I and ^{133}I [7,9], Valiente-Dobón *et al.* [10] have suggested the presence of new isomers with half-lives in the nanosecond range, although they have not provided detailed level schemes. The adjacent even-mass $_{52}$Te and $_{54}$Xe nuclides exhibit 7^- and 10^+ isomeric states [11,12], which are associated with two-neutron-hole configurations, $\nu h_{11/2}^{-1} d_{3/2}^{-1}$ and $\nu h_{11/2}^{-2}$, respectively, coupled to inactive proton pairs, $(\pi^2)_{0^+}$. The analogous isomers have also been identified in the $_{50}$Sn isotopes [13], but the observed $B(E2; 10^+ \rightarrow 8^+)$ values in the Te nuclei are much larger than those in their Sn isotones. Genevey *et al.* [11] ascribed this enhancement to the mixing of proton 2^+ components into the 8^+ and 10^+ wave functions. In the case of odd-Z isotopes, the unpaired proton couples to the neutron-hole states through effective interactions and induces strong configuration mixing of this kind via core polarization. The presence of a $23/2^+$ isomeric state in ^{129}Sb$_{78}$ and ^{131}Sb$_{80}$ ($Z = 51$) provides experimental evidence for a specific proton-particle and neutron-hole configuration of the type $\pi g_{7/2} \nu h_{11/2}^{-2}$ [14]. Whether such simple quasiparticle states persist with the addition of two protons or whether collective excitation patterns emerge are questions worth investigating. Spectroscopic information on ^{131}I and ^{133}I also serves as a test of the validity of a shell-model treatment in the case that a strong particle-hole repulsion exists in a multi-quasiparticle system.

II. EXPERIMENTAL PROCEDURES

Experimental studies of high-spin states in ^{131}I and ^{133}I were carried out at the ATLAS facility at Argonne National Laboratory. Various targets, such as the most neutron-rich stable Yb, Lu, W, and Os isotopes, were bombarded by ^{136}Xe beams at energies ranging from 6.0 to 6.2 MeV/nucleon, with

*Present address: Nuclear Physics Research Division, RIKEN Nishina Center, 2-1 Hirosawa, Wako, Saitama 351-0198, Japan; Corresponding author: hiroshi@ribf.riken.jp

†Present address: Department of Physics, University of Jyväskylä, P.O. Box 35 (YFL), 40014 Jyväskylä, Finland.

TABLE I. Summary of experimental conditions used in the analysis of the present work.

Target	Thickness (mg/cm^2)	Au backing (mg/cm^2)	Condition of ^{136}Xe beams	
			Energy (MeV)	Beam pulsing ON/OFF
^{176}Yb	6.4	25	820	1 ns/825 ns
^{176}Lu[a]	6.0	25	820	1 ns/825 ns
				10 μs/40 μs
				20 μs/60 μs
^{186}W	6.0	25	840	1 ns/825 ns
^{192}Os	44	10	840	1 ns/825 ns

[a]Lu enriched to 47% in ^{176}Lu.

TABLE II. Details of the pairwise combinations from 98 detectors used for the angular correlation analysis in the present work. The average, minimum, and maximum angular differences in degrees as well as the number of detector combinations used for each correlation matrix are listed.

Data point	$\Delta\theta_{av}$	$\Delta\theta_{min}$	$\Delta\theta_{max}$	Number of pairs
1	0.0	0.0	0.0	44
2	20.3	20.1	20.9	481
3	34.8	32.8	36.0	482
4	40.6	40.2	41.8	426
5	53.2	49.0	54.7	858
6	60.7	60.0	61.9	377
7	68.9	67.0	70.9	478
8	73.3	72.0	74.4	658
9	80.4	80.0	82.0	334
10	87.8	86.4	90.0	615

the primary purpose of studying relatively neutron-rich nuclei near the target isotopes [15–18]. The targets were composed of metallic foils on Au backings, thick enough to stop the majority of reaction products at the target position. The effective beam energies range from about 20% above the Coulomb barrier at incidence to near the barrier at the rear of the targets. Under these conditions, a large number of fragments are produced through complex nuclear reactions, including multinucleon transfer between the projectile and target nuclei as well as fusion-fission processes [19]. Because isomeric states in ^{131}I and ^{133}I were observed with all of the targets, all data sets were in principle useful for the analysis. The details of the targets used in the analysis of the present work are summarized in Table I.

The γ rays were detected with the Gammasphere spectrometer [20], in which 98 Compton-suppressed Ge detectors were operational. Most of the measurements were carried out with nanosecond-pulsed beams separated by 825 ns and with the coincidence requirement that three or more Ge detectors fired. The coincidence data sets were sorted into γ-γ-γ cubes, two-dimensional γ-γ matrices in coincidence with specific γ rays with appropriate relative and absolute time conditions, and also into ten γ-γ angular correlation matrices that were used to deduce transition multipolarities and determine the values of spins and parities. The number of detector combinations and the sets of angles that characterize the respective angular correlation matrices are summarized in Table II, where the value of $\Delta\theta_{av}$ is calculated by taking the weighted average of angular differences between pairs contained in each data point from $\Delta\theta_{min}$ to $\Delta\theta_{max}$. The number of detector pairs included in each correlation matrix ranges from 334 to 858, except for point 1, for which there are only 44 pairs. The data for this point is sometimes excluded from the angular correlation analysis, because its statistics are often too low to be reliable. The present selection provides a good compromise between the number of correlation points and obtaining reasonable statistics.

Additional measurements were carried out using macroscopically chopped beams with various beam on/off conditions. In these measurements, the coincidence requirements were relaxed to include events of twofold and higher, and data were only collected during the beam-off period. The decay of long-lived isomers was investigated by analyzing γ-γ matrices

created with gates on sequential time cuts in the out-of-beam region. The conditions of the beam pulsing used in the present analysis are also listed in Table I.

III. DATA ANALYSIS AND RESULTS

Figure 1 exhibits the level schemes for ^{131}I and ^{133}I established in the present work. Spin-parity assignments are based on the measured γ-γ angular correlations and total internal conversion coefficients. The results of angular correlation analysis and the deduced multipole mixing ratios are summarized in Table III.

A. ^{131}I

The 15/2$^-$ isomer at 1796 keV was previously reported with a half-life of 5.9 ns [7]. In the present work, a new isomeric state has been identified at 1918 keV. The coincidence spectra in Figs. 2(a) and 2(b) demonstrate that this isomer decays by a 122 keV transition to the known 15/2$^-$ isomeric state. Figure 2(d) displays time distributions of the 122 and 330 keV γ rays measured in coincidence with either the 782 or 773 keV γ rays in ^{131}I. A least-squares fit of the respective data yields nearly identical half-lives for the two transitions, allowing the 330 keV transition to be placed in parallel with the 122 keV γ ray, and implying an unobserved transition of 33 keV. The half-life of the 1918 keV isomeric state was determined to be 24(1) μs by taking a weighted average of the respective fits. The results of the angular correlation analysis indicate that the 122 and 330 keV transitions are of pure stretched quadrupole and dipole character, respectively (see the first and second rows in Table III). The total internal conversion coefficient for the 122 keV transition derived from the intensity balance analysis is $\alpha_T^{exp} = 0.85(7)$, which is in good agreement with the theoretical value for an $E2$ multipolarity ($\alpha_T^{cal} = 0.868$ [21]). Therefore, the spin and parity of the 24 μs isomeric state at 1918 keV is assigned as $J^\pi = 19/2^-$.

In addition to the decays from the 24 μs isomer, a number of new γ rays were observed in the out-of-beam region. They are identified in the spectrum obtained with a double gate on the known 782 and 773 keV lines in ^{131}I, as seen in Fig. 2(a).
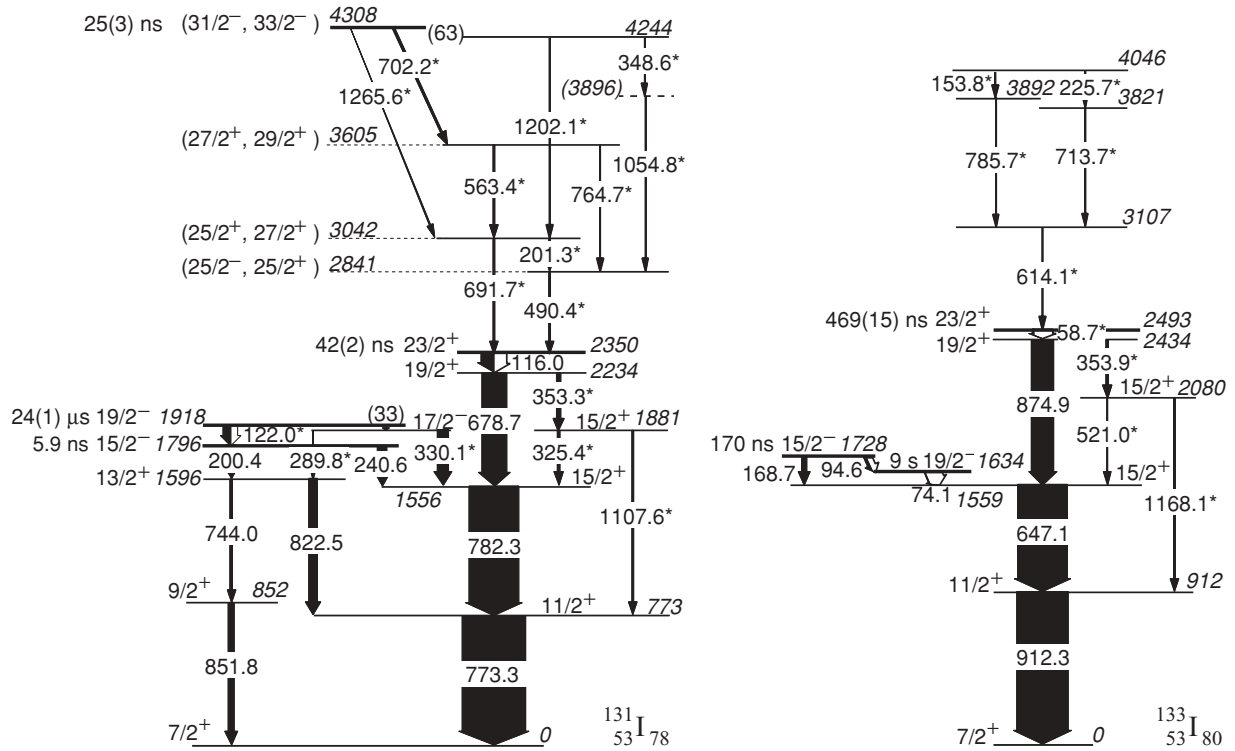
FIG. 1. Level schemes of ^{131}I and ^{133}I established in the present work. The widths of arrows represent relative intensities of γ rays extracted in the out-of-beam time regions, except for the transitions above the 2493 keV isomeric state in ^{133}I that were observed in the in-beam time region. Transitions observed for the first time are denoted with asterisks.

A careful investigation of the relative intensities and the coincidence relationships for the gated γ rays reveals that there are two more isomeric states in cascade. While Valiente-Dobón *et al.* [10] suggested the presence of a nanosecond isomer at 2352 keV, we identified this state to be located at 2350 keV, with decays via the 116–679 keV cascade followed by the 782 and 773 keV transitions. The γ rays populating this isomeric state have been identified in delayed coincidence with the 679,

TABLE III. Results of γ-ray angular correlation analysis for transitions in ^{131}I and ^{133}I.

Nucleus	E_γ (keV)	Angular correlation		Assignment for γ_2			Assignment for γ_1		
	γ_1-γ_2	A_{22}	A_{44}	Spin-parity	$\sigma\lambda$	$\delta(\lambda, \lambda+1)$	Spin-parity	$\sigma\lambda$	$\delta(\lambda, \lambda+1)$
^{131}I	122.0–782.3	0.164(66)	0.078(94)	$15/2^+ \to 11/2^+$	$E2$	0.0, fixed	$19/2^- \to 15/2^-$	$E2$	0.15^{+24}_{-16}
	330.1–782.3	−0.112(20)	0.005(30)	$15/2^+ \to 11/2^+$	$E2$	0.0, fixed	$17/2^- \to 15/2^+$	$E1$	−0.07(3)
	678.7–782.3	0.120(22)	0.022(33)	$15/2^+ \to 11/2^+$	$E2$	0.0, fixed	$19/2^+ \to 15/2^+$	$E2$	0.04(5)
	116.0–678.7	0.121(29)	0.017(42)	$19/2^+ \to 15/2^+$	$E2$	0.0, fixed	$23/2^+ \to 19/2^+$	$E2$	0.04(7)
	325.4–782.3	0.228(31)	0.000(44)	$15/2^+ \to 11/2^+$	$E2$	0.0, fixed	$15/2^+ \to 15/2^+$	$M1$	-0.23^{+22}_{-23}
	1107.6–773.3	0.126(63)	−0.005(90)	$11/2^+ \to 7/2^+$	$E2$	0.0, fixed	$15/2^+ \to 11/2^+$	$E2$	0.05^{+16}_{-13}
	563.4–691.7	0.256(91)	−0.01(13)	$25/2^+ \to 23/2^+$	$M1$	0.49^{+27}_{-8}	$27/2^+ \to 25/2^+$	$M1$	0.6, fixed
				$27/2^+ \to 23/2^+$	$E2$	0.0, fixed	$29/2^+ \to 27/2^+$	$M1$	0.99^{+35}_{-26}
	702.2–563.4	0.160(69)	−0.033(99)	$27/2^+ \to 25/2^+$	$M1$	0.58^{+30}_{-15}	$31/2^- \to 27/2^+$	$M2$	0.0, fixed
				$29/2^+ \to 27/2^+$	$M1$	0.57^{+30}_{-15}	$33/2^- \to 29/2^+$	$M2$	0.0, fixed
^{133}I	874.9–647.1	0.112(25)	0.012(36)	$15/2^+ \to 11/2^+$	$E2$	0.0, fixed	$19/2^+ \to 15/2^+$	$E2$	0.02^{+6}_{-5}
	521.0–647.1	0.269(94)	0.16(13)	$15/2^+ \to 11/2^+$	$E2$	0.0, fixed	$15/2^+ \to 15/2^+$	$M1$	-0.33^{+59}_{-67}
	1168.1–912.3	0.16(14)	0.24(19)	$11/2^+ \to 7/2^+$	$E2$	0.0, fixed	$15/2^+ \to 11/2^+$	$E2$	0.1^{+53}_{-3}

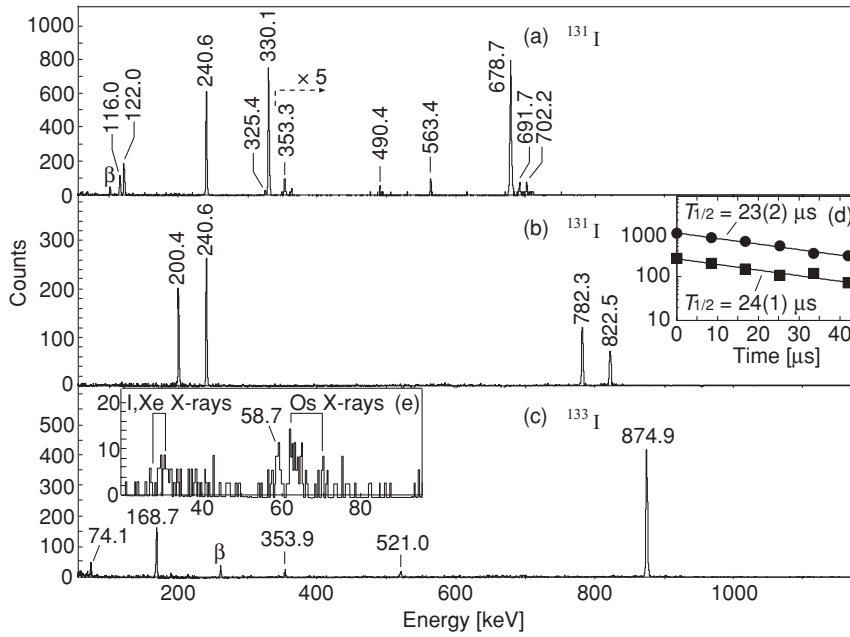FIG. 2. γ-ray coincidence spectra measured in the out-of-beam time region with (a) a double gate on the 782 and 773 keV transitions in ^{131}I; (b) a double gate on the 122 and 773 keV transitions in ^{131}I; and (c) a double gate on the 647 and 912 keV transitions in ^{133}I, using the ^{176}Yb target. In panel (a), the spectrum is multiplied by a factor of five at γ-ray energies higher than 350 keV. Panel (d) shows the time distributions of γ rays at 122 keV (solid squares) and at 330 keV (solid circles) in coincidence with either the 782 or 773 keV transition in ^{131}I. Panel (e) shows the low-energy spectrum obtained with the ^{192}Os target, with a double gate on the 875 and 647 keV transitions in ^{133}I. γ rays following the β decays are marked with β.
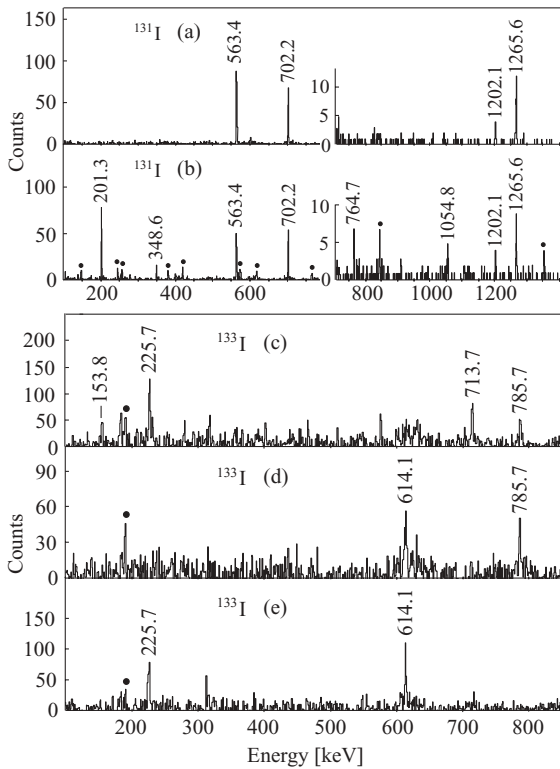

FIG. 3. γ-ray coincidence spectra preceding the $23/2^+$ isomeric states in ^{131}I and ^{133}I. The upper panels show γ rays measured in the out-of-beam period with coincidence gates on (a) the 692 keV and (b) 490 keV γ rays on γ-γ matrices created by gating on the delayed 679, 782, and 773 keV transitions in ^{131}I. The lower panels show prompt γ rays with coincidence gates on (c) the 614 keV, (d) 154 keV, and (e) 714 keV γ rays on γ-γ matrices created by gating on the delayed 875, 647, and 912 keV transitions in ^{133}I. Contaminant transitions are marked with solid circles.

782, and 773 keV transitions (see the upper panels of Fig. 3). Figure 4(a) illustrates the time difference spectrum between the 490/679 keV and 490/782 keV pairs of γ rays together with a fit resulting in a half-life of 42(2) ns, in good agreement with the value of 43(1) ns reported in Ref. [10]. The angular correlation analysis indicates a pure $E2$ character for both the 116 and 679 keV transitions, leading to an assignment of $23/2^+$ for the 2350 keV isomeric state. This result is supported by the total conversion coefficient derived for the 116 keV transition of $\alpha_T^{\rm exp} = 1.3(2)$, which is consistent with an $E2$ multipolarity ($\alpha_T^{\rm cal} = 1.04$ [21]).

Below the $23/2^+$ isomer, new decay cascades from the $19/2^+$ level have been identified via a state at 1881 keV. A spin-parity of $15/2^+$ was assigned for this intermediate level based on the measured angular correlations (Table III).

New levels above the $23/2^+$ isomer in ^{131}I were identified by analyzing γ-γ coincidence matrices created in the out-of-beam period with gates on the delayed 679, 782, and 773 keV transitions. The γ rays preceding the isomeric state are shown in Figs. 3(a) and 3(b). Another new isomer was identified at 4308 keV, decaying by 702 and 1266 keV transitions. Furthermore, the observation of the 1202 keV γ ray and the 349–1055 keV cascade (the order of the latter transitions is ambiguous) parallel to the main isomeric decay branches suggests the presence of an unobserved 63 keV transition from the 4308 keV state. The relative intensities for the isomeric transitions are listed in Table IV. A half-life of 25(3) ns has been deduced from a least-squares fit of the time spectrum obtained with a double gate on the 702 and 563 keV γ rays [Fig. 4(b)].

The angular correlations between the γ rays feeding and deexciting the $23/2^+$ state were found to be isotropic, presumably because of the attenuation of the alignment at the intermediate $T_{1/2} = 42$ ns isomeric state. Therefore, spins and parities for the 2841 and 3042 keV levels could not be
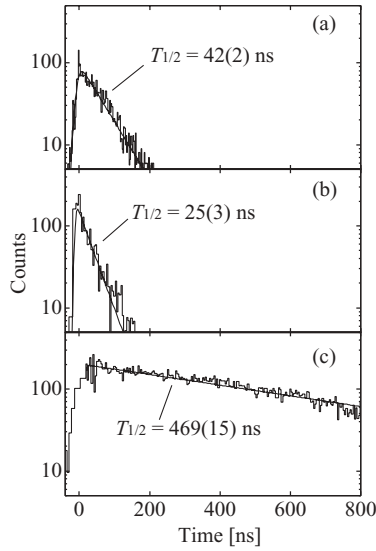
FIG. 4. Time spectra in the nanosecond range and associated fits for γ rays in ^{131}I and ^{133}I. Panel (a) shows the sum of two time difference spectra between the 490/679 keV and 490/782 keV pairs of transitions in ^{131}I, measured in the out-of-beam period. Panels (b) and (c) show the time distributions of γ-γ coincidence events relative to the beam pulse measured with a double gate on the 702/563 keV transitions in ^{131}I and on the 875/647 keV transitions in ^{133}I, respectively. For the fits, an exponential convoluted with a Gaussian function was used in each case.

determined. Given the lack of expected decays to the $19/2^+$ state at 2234 keV and to the $19/2^-$ state at 1918 keV via possible $E2$ transitions, the spins of these two levels must be $J > 23/2$. Furthermore, if the 2841 keV state had the same spin and parity as the 3042 keV level, the 4308 keV isomeric state would prefer to decay toward the lower level rather than toward the higher one. Assuming that the spin increases with excitation energy along the yrast cascades, and that the prompt γ-ray emissions are of $E1$, $M1$, or $E2$ character, except for low-energy transitions, the 2841 keV state most likely has a spin of 25/2 and there remains a possible spin-parity assignment for the 3042 keV level of $25/2^{\pm}$ or $27/2^+$ depending on the parity assigned to the 2841 keV state.

With deduced total transition intensities for the three branches from the $T_{1/2} = 25$ ns isomeric state at 4308 keV, the transition strengths for all possible multipolarities are evaluated in Table IV. For the 702 and 1266 keV transitions, the total transition intensity, including conversion, is essentially

equivalent to the relative intensity of each γ ray because the conversion coefficients will be small, while the total transition intensity for the 63 keV transition was derived from the sum of the γ-ray intensities of the 1202 and 1055 keV transitions from the 4244 keV state, as measured in the out-of-beam time period. The transition strengths in Table IV virtually rule out all $\Delta J \geqslant 3$ possibilities for the 702 keV transition, and dipole transitions are unlikely to occur as the main decay branch given the large hindrances implied. Thus, this transition is likely to have a quadrupole multipolarity. Similar arguments lead to the suggestion of either $M2$ or $E3$ character for the 1266 keV transition. These arguments also imply that the spin changes by one unit at most through the 563 keV transition.

The γ-γ angular correlations were successfully extracted for the 563–692 keV and 702–563 keV cascades in ^{131}I (see Table III). In the analysis of angular correlations, the mixing ratio of one of the coincident γ rays can be derived from the experimental values of the A_{22} and A_{44} coefficients by fixing the mixing ratio of the other. It is reasonable to assume the multipole radiations to be pure except for $M1$ transitions. The mixing ratio of a $M1$ transition is fixed to a finite value if it is independently known. For instance, the mixing ratio of 0.6(2), that was derived from the angular correlation between the 702 and 563 keV transitions, is assumed for a 563 keV, $27/2^+ \rightarrow 25/2^+$ ($M1 + E2$) transition in the analysis of the 563–692 keV correlation. With this constraint on the multipole mixing ratio and with the measured values of A_{22} and A_{44}, one can exclude not only the spin sequences for which there are no minima for the mixing ratio in the χ^2 distribution (below the 5% confidence level) but also the cases in which mixed $E1$ or $E2$ transitions are involved. For example, an assignment of $25/2^{\pm} \rightarrow 25/2^- \rightarrow 23/2^+$ for the 563–692 keV cascade can be eliminated from the possible spin sequences because a fit of the observed A_{22} and A_{44} does not give a minimum in the χ^2 for the mixing ratio of the 563 keV transition when assuming that the 692 keV transition is of pure $E1$ character. Although a similar fit to a $27/2^{\pm} \rightarrow 25/2^- \rightarrow 23/2^+$ sequence yields a mixing ratio of $-1.2(7)$ for the 563 keV transition, indicating mixed $M1 + E2$ character, this value of the mixing ratio is inconsistent with that obtained from the 702–563 keV correlation (see Table III). Therefore, the assignment of $J^\pi = 25/2^-$ for the 3042 keV level can be excluded from the possible spin-parity assignments. However, the values of $J^\pi = 25/2^+$ and $27/2^+$ are allowable for the 3042 keV state, provided that $M1 + E2$ mixed multipole transitions are involved in the 563–692 keV cascade.

TABLE IV. $B(\sigma\lambda)$ values for transitions depopulating the $T_{1/2} = 25(2)$ ns isomeric state in ^{131}I, assuming different multipolarities.

E_γ (keV)	I_{tot}[a] (relative)	$B(\sigma\lambda)$ (W.u.)					
		$E1$	$M1$	$E2$	$M2$	$E3$	$M3$
63	11(2)	2.6×10^{-6}	9.8×10^{-5}	6.0	1.2×10^2	5.9×10^6	2.0×10^8
702.2	70(5)	2.1×10^{-8}	1.7×10^{-6}	2.3×10^{-3}	0.19	3.9×10^2	5.2×10^2
1265.6	19(3)	9.4×10^{-10}	7.9×10^{-8}	3.2×10^{-5}	2.7×10^{-3}	1.7	1.4×10^2

[a]$I_{\text{tot}} = I_\gamma(1 + \alpha_T)$. See Sec. III A.

Based on the above assumptions and arguments on the expected spin-parity assignment for the levels between the 2350 and 4308 keV in ^{131}I, the spins and parities are assigned as $31/2^- \rightarrow 27/2^+ \rightarrow 25/2^+ \rightarrow 23/2^+$ or $33/2^- \rightarrow 29/2^+ \rightarrow 27/2^+ \rightarrow 23/2^+$ for the 702–563–692 keV cascade, with derived mixing ratios as summarized in Table III. It can be seen that the 25 ns isomer at 4308 keV most likely has negative parity with a spin of either 31/2 or 33/2$\hbar$.

B. ^{133}I

Previously studied levels in ^{133}I include the $15/2^-$, 1728 keV isomeric state with a half-life of 170 ns [9] and the $T_{1/2} = 9$ s isomer at 1634 keV [22]. The spin and parity of the 9 s isomer has been determined to be $19/2^-$, based on the measured total conversion coefficient for the 74 keV $M2$ transition [9]. This level is the analog of the $19/2^-$ isomeric state in ^{131}I, which was identified in the present work (see preceding section).

In ^{133}I, a level at 2436 keV has been suggested to be an isomeric state with a half-life of 780(160) ns in the preliminary work of Ref. [10]. From the present spectroscopic results, the 2434 keV state is assigned as $J^\pi = 19/2^+$, implying that the 875 keV $E2$ deexcitation would be extremely hindered if this level were the isomer. Figure 2(e) presents a low-energy spectrum observed with a dual gate on the 875 and 647 keV γ rays in the out-of-beam period. A γ-ray peak at 59 keV can be isolated from the x rays in the spectrum obtained with the ^{192}Os target. The γ-ray intensity balance analysis for the 59 keV transition results in a total conversion coefficient $\alpha_T^{exp} = 19(4)$, to which a theoretical prediction for an $E2$ multipolarity ($\alpha_T^{cal} = 11.9$ [21]) is closest. Thus, it is concluded that there is a new 2493 keV isomeric level in ^{133}I, the analog of the $23/2^+$ isomeric state in ^{131}I. The half-life of this isomeric state was determined to be 469(15) ns, as shown in Fig. 4(c).

A second $15/2^+$ state has been identified at 2080 keV, populated in the decay path from the $23/2^+$ isomeric state in ^{133}I, similar to decays in ^{131}I. In ^{133}I, however, no indication of isomeric states above the $23/2^+$ isomer has been found in the coincidence spectra observed in the out-of-beam period. Nevertheless, several prompt transitions were observed to precede the γ decays out of the 469 ns isomeric state, as indicated in the lower panels of Fig. 3. The 614 keV transition, which was observed prominently in all the data sets with different targets, is placed just above the $23/2^+$ isomeric state in ^{133}I, and by gating on this transition, two parallel cascades stemming from a common 4046 keV level were identified. The order of these γ rays was determined from their relative prompt intensities. Firm spin-parity or multipolarity assignments were not possible, but the 4046 keV state must have $J \sim 31/2$.

IV. DISCUSSION

To understand the observed level properties of ^{131}I and ^{133}I, a shell-model calculation based on a j-j coupling scheme was performed. The model space considered in the present calculation is the 50-82 shell, including all five available orbits for neutron holes, but only the $g_{7/2}$ and $d_{5/2}$ subshells for

protons. With the doubly magic nucleus ^{132}Sn as a closed core, the basis states can be described as $|(\pi^3)_{J_p} \otimes (\nu^{-x})_{J_n}; J\rangle$ with $x = 4$ for ^{131}I and $x = 2$ for ^{133}I. The single-particle energies are taken from the experimental levels of ^{133}Sb [23] and ^{131}Sn [24] for the valence protons and neutron holes, respectively. The surface-delta interaction (SDI) is employed for the p-p and n-n interactions, that were adjusted to reproduce the observed level energies of ^{134}Te and ^{130}Sn, respectively. The p-n matrix elements were derived from the Schiffer-True interaction [25] in the particle-hole formalism.

Figure 5 provides the comparison between the calculated and observed levels in ^{131}I and ^{133}I, together with the ^{130}Te levels with experimental values from Ref. [26]. Up to the $23/2^+$ isomeric states, the present calculation reproduces the experimental level energies within the RMS deviations of 54 and 47 keV for ^{131}I and ^{133}I, respectively, and illustrates the similarity of the level structures in ^{131}I and ^{133}I. For instance, there are two $15/2^+$ states in both iodine isotopes. The shell-model calculation suggests that the first $15/2^+$ state is dominated by proton excitations of the type $(\pi^3)_{15/2^+}$ coupled to an inactive $(\nu^{-x})_{0^+}$ component. This prediction is supported by the fact that the $15/2_1^+$ energy is slightly higher in ^{131}I and ^{133}I than in the $N = 82$ single-closed nucleus ^{135}I ($E_x = 1422$ keV [4]), similar to the observation for the 6^+ states in Te isotopes arising from the aligned $\pi g_{7/2}^2$ configuration [4,11].

The $19/2^-$ and $23/2^+$ isomeric states are expected to involve predominantly two-neutron-hole excitations because alternative states arising from the $(\pi g_{7/2}^2 h_{11/2})_{19/2^-}$ and $(\pi g_{7/2}^3 \nu f_{7/2} h_{11/2}^{-1})_{23/2^+}$ configurations are much higher in energy, being at 3655 and 4776 keV, respectively, in ^{135}I [4]. The shell-model calculation indicates that the wave function of the $19/2^-$ state consists predominantly of a proton seniority-one and neutron seniority-two component $|\pi g_{7/2} \otimes (\nu h_{11/2}^{-1} d_{3/2}^{-1})_{7^-}; 19/2^-\rangle$ (68.4% in ^{133}I and 55.7% in ^{131}I). The strong particle-hole repulsion raises the energy for the maximum spin coupling of a $|(\pi)_{J_p} \otimes (\nu_1^{-1} \nu_2^{-1})_{J_n}; J\rangle$ three-quasiparticle multiplet, so that the $J = J_{max} - 1$ member falls lower in energy. The observation of this feature for the $19/2^-$ isomeric state in ^{131}I suggests that a spin coupling of this type still occurs in multi-quasiparticle configurations that involve π^2 and ν^{-2} pairs coupled to spin zero.

In ^{129}Sb and ^{131}Sb, the $23/2^+$ isomeric state is interpreted as being associated predominantly with the $J_{max} - 2$ member of the $\pi g_{7/2}(\nu h_{11/2}^{-2})_{10^+}$ multiplet [14]. The experimental $B(E2)$ values for the $10^+ \rightarrow 8^+$ transitions in the Sn and Te isotopes and for the $23/2^+ \rightarrow 19/2^+$ transitions in the Sb and I isotopes with $N = 78$ and 80 are listed in Table V. It can be seen that the $E2$ transition strength increases when moving away from the $Z = 50$ and $N = 82$ shell closures. According to the shell-model calculation, the wave function of the $23/2^+$ state in ^{131}I and ^{133}I consists of many components, including seniority-three π^3 excitations, and the constituent protons and neutrons coherently contribute to the $E2$ matrix element, giving rise to the collectivity. This would be the underlying cause for the observed enhancement of the $B(E2; 23/2^+ \rightarrow 19/2^+)$ values in the iodine isotopes. The calculated transition strengths of the $E2\gamma$ rays depopulating the positive-parity isomers in the $N = 78, 80$ isotones are compared with the experimental
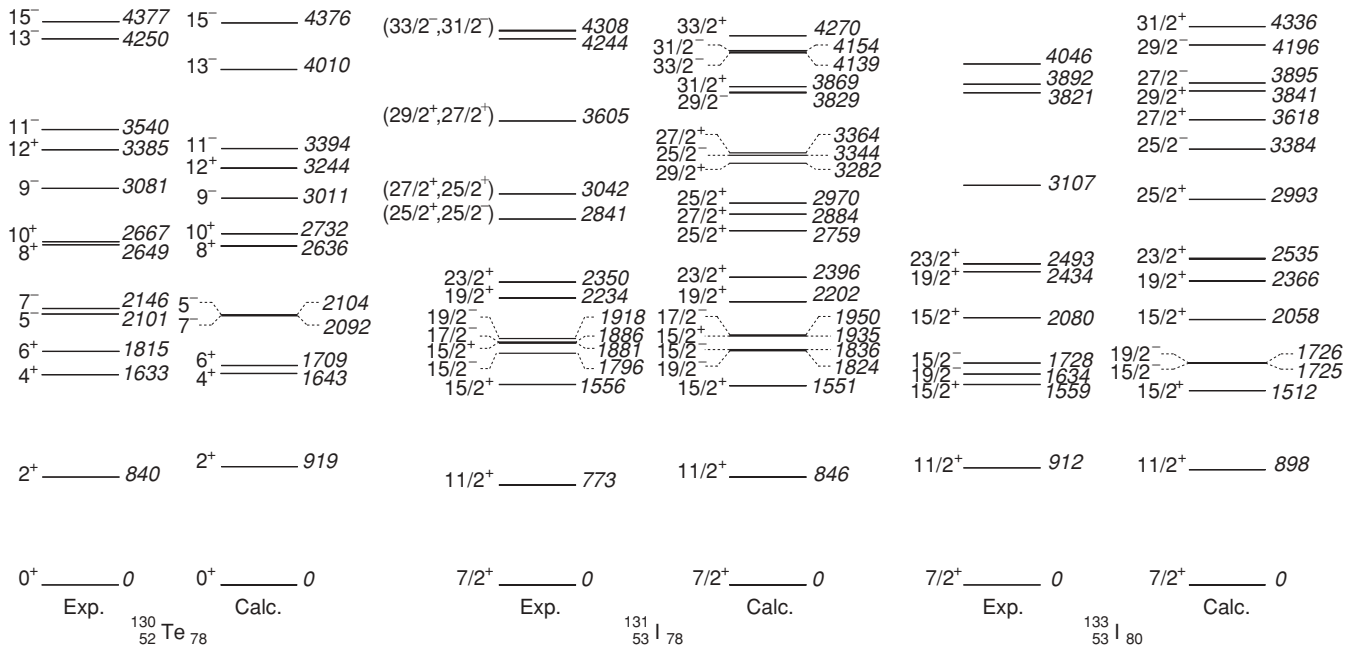
130/52 Te 78 — Exp.
15⁻ 4377; 13⁻ 4250; 11⁻ 3540; 12⁺ 3385; 9⁻ 3081; 10⁺ 2667; 8⁺ 2649; 7⁻ 2146; 5 2101; 6⁺ 1815; 4⁺ 1633; 2⁺ 840; 0⁺ 0

130/52 Te 78 — Calc.
15⁻ 4376; 13⁻ 4010; 11⁻ 3394; 12⁺ 3244; 9⁻ 3011; 10⁺ 2732; 8⁺ 2636; 5⁻ 2104; 7⁻ 2092; 6⁺ 1709; 4⁺ 1643; 2⁺ 919; 0⁺ 0

131/53 I 78 — Exp.
(33/2⁻,31/2⁻) 4308, 4244; (29/2⁺,27/2⁺) 3605; (27/2⁺,25/2⁺) 3042; (25/2⁺,25/2⁻) 2841; 23/2⁺ 2350; 19/2⁺ 2234; 19/2⁻ 1918; 17/2⁺ 1886; 15/2⁺ 1881; 15/2⁻ 1796; 15/2⁺ 1556; 11/2⁺ 773; 7/2⁺ 0

131/53 I 78 — Calc.
33/2⁺ 4270; 31/2⁻ 4154; 33/2⁻ 4139; 31/2⁺ 3869; 29/2⁻ 3829; 27/2⁺ 3364; 25/2⁻ 3344; 29/2⁺ 3282; 25/2⁺ 2970; 27/2⁺ 2884; 25/2⁺ 2759; 23/2⁺ 2396; 19/2⁺ 2202; 17/2⁻ 1950; 15/2⁺ 1935; 15/2⁻ 1836; 19/2⁻ 1824; 15/2⁺ 1551; 11/2⁺ 846; 7/2⁺ 0

133/53 I 80 — Exp.
4046; 3892; 3821; 3107; 23/2⁺ 2493; 19/2⁺ 2434; 15/2⁺ 2080; 15/2⁻ 1728; 19/2⁻ 1634; 15/2⁺ 1559; 11/2⁺ 912; 7/2⁺ 0

133/53 I 80 — Calc.
31/2⁺ 4336; 29/2⁻ 4196; 27/2⁻ 3895; 29/2⁺ 3841; 27/2⁺ 3618; 25/2⁻ 3384; 25/2⁺ 2993; 23/2⁺ 2535; 19/2⁺ 2366; 15/2⁺ 2058; 19/2⁻ 1726; 15/2⁻ 1725; 15/2⁺ 1512; 11/2⁺ 898; 7/2⁺ 0

FIG. 5. Experimental and calculated energies in keV for the selected states in ^{131}I, ^{133}I, and ^{130}Te. The experimental values for the ^{130}Te levels are adopted from Ref. [26].

values in Table V. In this calculation, an effective proton charge of $1.55e$ which reproduces the observed $B(E2; 6^+ \to 4^+)$ value in ^{134}Te [4] was adopted, as was a value of $0.82e$ for neutron holes so as to reproduce the experimental value of $B(E2; 10^+ \to 8^+)$ in ^{130}Sn [13]. Although the calculation somewhat overestimates the $B(E2; 23/2^+ \to 19/2^+)$ value for ^{131}I, it can be seen that the upward trend in the transition rates in the Te and I isotopes as the proton number increases and neutrons are removed from the $N = 82$ shell closure is qualitatively accounted for.

It is expected that proton seniority-three and neutron seniority-two components $|(\pi^3)_{J_p} \otimes (\nu h_{11/2}^{-2})_{J_n}; J^+\rangle$ mainly contribute to the formation of positive-parity states above the $23/2^+$ isomer. The shell-model calculation predicts stretch-aligned configurations of the type $(\pi g_{7/2}^3 \nu h_{11/2}^{-2})_{35/2^+}$ and $(\pi g_{7/2}^2 d_{5/2} \nu h_{11/2}^{-2})_{37/2^+}$ to lie at 5498 and 6136 keV, respectively, in ^{133}I, i.e., much higher than the observed 4046 keV level. The predictions for positive-parity states at high spins are also given in Fig. 5. The comparison of the experimental and calculated level energies, as well as the observed level

sequences between the 2493 and 4046 keV states in ^{133}I, suggests that the 4046 keV level would have $J \sim 31/2$.

Finally, it is noteworthy that the high-spin isomer with either $J^\pi = 33/2^-$ or $31/2^-$ in ^{131}I has no known equivalent in ^{129}Sb and ^{131}Sb, or in ^{133}I. States at $31/2^-$ and $33/2^-$ are predicted by the present shell-model calculation with the leading term of the wave function in both cases involving a neutron seniority-four component $(\nu h_{11/2}^{-3} d_{3/2}^{-1})_{15^-}$, the same as that assigned to the 15^- isomeric state in ^{130}Te [26]. Here, a $37/2^-$ level, which is likely to arise from the maximum spin coupling of the 15^- state with an odd proton in the $g_{7/2}$ orbit, is expected to appear above 5 MeV. The observed isomeric state at 4308 keV in ^{131}I decays by possible transitions with $M2$ (0.19 W.u. for the 702 keV transition) and $E3$ (1.7 W.u. for the 1266 keV transition) multipolarities, presumably implying the admixture of different multiplets including the $h_{11/2}$ protons in the initial and final states. Such $M2$ and $E3$ transitions from the $11/2^-$ state to the lower-lying $7/2^+$ and $5/2^+$ levels are also observed in the odd-A Sb isotopes with $A = 115$–123 [27–29]. Although the $h_{11/2}$ proton orbit

TABLE V. $B(E2)$ values for transitions deexciting the positive-parity isomers in the $Z = 50$–53 isotopes with $N = 78$ and 80.

Z	$J_i^\pi \to J_f^\pi$	$B(E2)$ in $N = 78$ (e^2 fm^4)			$B(E2)$ in $N = 80$ (e^2 fm^4)		
		Calc.	Exp.	Ref.	Calc.	Exp.	Ref.
$_{50}$Sn	$10^+ \to 8^+$	4.2	14.4(13)	[13]	14.5	14.5(14)	[13]
$_{51}$Sb	$23/2^+ \to 19/2^+$	15.2	20(2)	[14]	27.3	21(4)	[14]
$_{52}$Te	$10^+ \to 8^+$	78.0	85(4)	[26]	52.0	43(2)	[11]
$_{53}$I	$23/2^+ \to 19/2^+$	455.9	314(14)	a	121.7	135(4)	a

[a]Present work.

is not taken into account in the present calculation, the excitation energy of the $31/2^-$ and $33/2^-$ states should not be much affected by the protons occupying this orbit, which lies 2.8 MeV above the $g_{7/2}$ orbit [23].

As shown in the decay scheme of ^{130}Te (see Fig. 3 of Ref. [26]), the 15^- isomer decays via a 127 keV, $E2$ transition to the 13^- state, followed by γ-ray cascades populating the lower-lying 10^+ and 7^- isomeric states. In the case of ^{131}I, a $29/2^-$ level is predicted to lie 310 keV below the $33/2^-$ state. The relative intensity for this branch is estimated to be about 10% by the present calculation. Thus, the decay from the 25 ns isomer might partially proceed through the $29/2^-$ level and subsequent negative-parity levels feeding the $19/2^-$ state. However, the presence of the 24 μs half-life could prevent us from observing such feeding transitions in coincidence with the γ rays depopulating the $19/2^-$ isomeric state.

V. CONCLUSIONS

We have studied the level structure of ^{131}I and ^{133}I up to excitation energies of about 4 MeV, using multinucleon transfer reactions between ^{136}Xe beams and thick targets. An isomeric state with $J^\pi = 19/2^-$, $T_{1/2} = 24(1)$ μs has been identified in ^{131}I, as well as nanosecond isomers with $J^\pi = 23/2^+$ in both isotopes. In addition, a high-spin isomer with a half-life of 25(3) ns has been identified at 4308 keV in

^{131}I. Based on the measured angular correlations and transition probabilities, this isomer most likely has $J^\pi = 31/2^-$ or $33/2^-$ quantum number.

The observed analogies between states in ^{131}I and ^{133}I suggest that the $19/2^-$ and $23/2^+$ isomeric states are dominated by two-neutron-hole configurations coupled to odd protons. A j-j coupling shell-model calculation reproduces the experimental level energies well and qualitatively explains the behavior of the observed $B(E2)$ values of the $10^+ \to 8^+$ transitions in Sn and Te isotopes and those of the $23/2^+ \to 19/2^+$ transitions in Sb and I isotopes with $N = 78$ and 80. The high-spin negative-parity isomer in ^{131}I most likely involves a proton coupled to the $(\pi^2)_{0^+}(\nu h_{11/2}^{-3} d_{3/2}^{-1})_{15^-}$, four-neutron-hole configuration, which is assigned to the 15^- isomeric state in ^{130}Te.

[1] R. E. Shroy, D. M. Gordon, M. Gai, D. B. Fossan, and A. K. Gaigalas, Phys. Rev. C **26**, 1089 (1982).
[2] M. Gai, D. M. Gordon, R. E. Shroy, D. B. Fossan, and A. K. Gaigalas, Phys. Rev. C **26**, 1101 (1982).
[3] W. F. Piel, P. Chowdhury, U. Garg, M. A. Quader, P. M. Stwertka, S. Vajda, and D. B. Fossan, Phys. Rev. C **31**, 456 (1985).
[4] C. T. Zhang *et al.*, Phys. Rev. Lett. **77**, 3743 (1996).
[5] S. K. Saha *et al.*, Phys. Rev. C **65**, 017302 (2001).
[6] C. Goodin *et al.*, Phys. Rev. C **78**, 044331 (2008).
[7] S. V. Jackson, W. B. Walters, and R. A. Meyer, Phys. Rev. C **11**, 1323 (1975).
[8] G. Lhersonneau, J. De Raedt, H. Van de Voorde, H. Ooms, R. Haroutunian, E. Schoeters, R. E. Silverans, and L. Vanneste, Phys. Rev. C **12**, 609 (1975).
[9] W. B. Walters, E. A. Henry, and R. A. Meyer, Phys. Rev. C **29**, 991 (1984).
[10] J. J. Valiente-Dobón *et al.*, Phys. Rev. C **69**, 024316 (2004).
[11] J. Genevey, J. A. Pinston, C. Foin, M. Rejmund, R. F. Casten, H. Faust, and S. Oberstedt, Phys. Rev. C **63**, 054315 (2001).
[12] A. Kerek, A. Luukko, M. Grecescu, and J. Sztarkier, Nucl. Phys. **A172**, 603 (1971).
[13] B. Fogelberg, K. Heyde, and J. Sau, Nucl. Phys. **A352**, 157 (1981).
[14] J. Genevey, J. A. Pinston, H. R. Faust, R. Orlandi, A. Scherillo, G. S. Simpson, I. S. Tsekhanovich, A. Covello, A. Gargano, and W. Urban, Phys. Rev. C **67**, 054312 (2003).

[15] G. D. Dracoulis *et al.*, Phys. Lett. **B584**, 22 (2004).
[16] G. D. Dracoulis *et al.*, Phys. Rev. C **71**, 044326 (2005).
[17] F. G. Kondev *et al.*, Eur. Phys. J. A **22**, 23 (2004).
[18] G. D. Dracoulis *et al.*, Phys. Lett. **B635**, 200 (2006).
[19] R. Broda, J. Phys. G: Nucl. Part. Phys. **32**, R151 (2006).
[20] I. Y. Lee, Nucl. Phys. **520**, c641 (1990).
[21] T. Kibédi, T. W. Burrows, M. B. Trzhaskovskaya, P. M. Davidson, and C. W. Nestor, Nucl. Instrum. Methods A **589**, 202 (2008).
[22] I. Bergstrom, G. Borg, G. B. Holm, and B. Rydberg, in *Proceedings of the International Conference on Properties of Nucleides far from the Region of β-Stability*, CERN-70-30, Vol. 2 (Leysin, Switzerland, 1970), p. 1012.
[23] M. Sanchez-Vega, B. Fogelberg, H. Mach, R. B. E. Taylor, A. Lindroth, J. Blomqvist, A. Covello, and A. Gargano, Phys. Rev. C **60**, 024303 (1999).
[24] B. Fogelberg *et al.*, Phys. Rev. C **70**, 034312 (2004).
[25] J. P. Schiffer and W. W. True, Rev. Mod. Phys. **48**, 191 (1976).
[26] R. Broda, B. Fornal, W. Krlas, T. Pawlstrokat, J. Wrzesinacuteski, D. Bazzacco, G. de Angelis, S. Lunardi, and C. Rossi-Alvarez, Eur. Phys. J. A **20**, 145 (2004).
[27] R. E. Shroy, A. K. Gaigalas, G. Schatz, and D. B. Fossan, Phys. Rev. C **19**, 1324 (1979).
[28] D. R. LaFosse, D. B. Fossan, J. R. Hughes, Y. Liang, H. Schnare, P. Vaska, M. P. Waring, and J.-Y. Zhang, Phys. Rev. C **56**, 760 (1997).
[29] H. Watanabe *et al.*, Phys. Rev. C **79**, 024306 (2009).